ORIGINAL ARTICLE

Drops in needle production are early-warning signals of drought-triggered dieback in Scots pine

Gabriel Sangüesa-Barreda[1] **· Antonio Gazol**[2] **· J. Julio Camarero**[2]

Abstract

Key message Reconstruction of needle dynamics reveals prolonged drought legacy effects on crown condition that represent early warnings of drought-induced dieback in Scots pine.

Abstract Understanding the mechanisms of drought-induced forest dieback and tree mortality is a priority for predicting forest responses to climate change. However, long-term information on drought impacts on crown dynamics and how it relates to tree water and carbon economy is still lacking. Comparing declining and non-declining Scots pines at the same site, we quantified primary and secondary growth and intrinsic water-use efficiency (WUE_i). Further, we reconstructed the needle production and the annual total number of needles using the Needle Trace Method. Here, we reconstructed the apical needles through the assessment of 2460 longitudinal sections. We fitted partial least squares regression models to assess climate influence on primary and secondary growth and needle dynamics, and then linear mixed models using climate covariates and discerning between health status in the 1975–2016 period. Finally, we analyzed drought legacy effects applying a Bayesian hierarchical framework. We detected the highest differences between health tree classes in the annual total number of needles during the warm-dry 1980s. Declining trees responded more negatively to climate than non-declining conspecifics and showed a higher variability of drought legacy effects. We found significant drought legacy effects in the annual total number of needles up to 3 years after a drought. The warm, dry 1980s, that preceded the dieback, showed the highest $\delta^{13}C$ values since the 1970s. Declining trees showed higher WUE_i than non-declining trees from the 2000s onwards. Our study sheds light on the major role of needle dynamics in dieback episodes and illustrates how past drops in needle production may be interpreted as early warnings of drought-induced dieback in Scots pine.

Keywords Crown dynamics · Needle trace method · *Pinus sylvestris* · Primary growth · Water-use efficiency

Introduction

Declining tree vitality and forest dieback are global responses to increasing evapotranspiration rates and severe droughts (Hartmann et al. 2022). Elevated tree mortality has significant repercussions on forest composition, structure, and function (Batllori et al. 2020), but also for global carbon and water cycles (Wang et al. 2012). Therefore, understanding the mechanisms underlying dieback and associated

✉ Gabriel Sangüesa-Barreda
gabriel.sanguesa@uva.es

1 EiFAB-iuFOR, Universidad de Valladolid, Campus Duques de Soria s/n, 42004 Soria, Spain

2 Instituto Pirenaico de Ecología (IPE-CSIC), Saragossa, Spain

tree mortality, as well as tree species' responses to hotter droughts, is a priority issue to tackle global warming impacts on forests (Allen et al. 2015; Dai 2013).

Trees close stomata in response to drought stress to limit water loss by transpiration, decreasing the risk of hydraulic failure but also limiting CO_2 uptake via photosynthesis and growth (Martin-StPaul et al. 2017; Pinheiro and Chaves 2011). Numerous empirical studies have investigated the interaction of the two proposed mechanisms of drought-induced tree mortality: hydraulic failure and carbon starvation (McDowell et al. 2022). For instance, McDowell et al. (2011) associated tree mortality to a gradual depletion of carbon reserves coupled with a steady hydraulic dysfunction. Adams et al. (2017) pointed out the ubiquitous reduction on xylem hydraulic conductivity due to widespread embolism as a major mechanism of mortality across species. Despite this mechanistic framework, deciphering the

causes of dieback and tree mortality in response to drought is rather hard (Trugman et al. 2021), partially because of the difficulty of tracing tree performance prior to drought occurrence.

In conifers, the development of shoot apical meristems and leaves usually occurs later than the development of vascular tissues (Michelot et al. 2012), demonstrating that cambium activity depends on stored non-structural carbohydrates (Fang et al. 2020), but also on temperature (Rossi et al. 2008), and soil water availability during tracheid enlargement (Cabon et al. 2020). Apical meristems and foliar development may also be affected by severe water scarcity (Bréda et al. 2006), with delayed responses of both crown condition and tree growth to drought stress (Bréda et al. 2006; Gazol et al. 2020). That is, foliar development can be temporally decoupled from radial growth (e.g., Kannenberg et al. 2019), and what we observe in tree rings might leave a previous imprint on the development of shoot apical meristems and leaves.

The drought-driven dieback process (e.g., from needle browning and shedding to tree mortality) may last from a few months to several decades depending on the species, the local climate settings, and the contribution of biotic stressors (Camarero et al. 2015a; Cailleret et al. 2017; DeSoto et al. 2020). The long-lasting impacts of successive severe droughts on carbon uptake and crown development could be one of the causes of these prolonged responses. Thus, early warning signals of tree dieback can be different depending on the organ considered, a question that should be further investigated. However, despite the interconnections between carbon sources and sinks, the strong influence of climate on primary and secondary growth over time, and the major role of needles as organs of carbon assimilation, sugar production, and water loss, they have been rarely analyzed at long-time scales probably due to the lack of reliable records of leaf production and radial growth. In other words, we lack reliable information on the matches and mismatches of these temporal trends and how they evolve in response to drought.

Several physiological traits associated with carbon uptake can be reconstructed over time. The most used proxies are tree-ring variables, which inform on the allocation of assimilates to secondary or radial growth (Fritts 1976). Dendroecological studies have advanced in the understanding of drought-induced mechanisms of tree mortality and the capacity of trees to deal with drought stress, particularly using hydraulics and functional traits, such as wood density, wood anatomy, or C and O stable isotope ratios (e.g., López et al. 2021; Cailleret et al. 2017; Martínez-Vilalta 2018). Other functional traits, such as the tree capacity to fix carbon from the air, that is, the needle retention or abundance among other factors, are much more difficult to quantify retrospectively. The Needle Trace Method allows reconstructing needle production by analyzing needle scars formed in the wood (Kurkela and Jalkanen 1990; Pensa and Jalkanen 2005). Until now, this technique has been mainly applied in cold-limited or temperate pine populations where needle retention correlates positively with latitude and air temperature (Jalkanen et al. 1995; Xiao 2003), while less is known about the needle dynamics in Mediterranean, water-limited pine populations.

Drought-induced drops in needle production could have long-lasting consequences on tree carbon and water economy (Salmon et al. 2015). Retrospectively, the carbon and water balance can be assessed as the ratio between photosynthesis (A) and stomatal conductance (gs) rates through the study of carbon isotope composition ($\delta^{13}C$) in tree rings and the calculation of the intrinsic water-use efficiency (i.e., the carbon gain per unit of water loss; WUE_i, or A/gs; cf. Farquhar et al. 1982). The WUE_i usually shows a positive trend because of rising atmospheric CO_2 levels by stimulating photosynthesis and reducing water loss through leaves (Saurer et al. 2014). In drought periods, WUE_i is also expected to increase due to stomatal closure and gs decrease. The combination of needle production dynamics and tree-ring WUE_i allows interpreting tree-level water and carbon economy by focusing on photosynthetic-related organs. For instance, a drop in needle production and a rise in WUE_i could be expected in response to drought.

In 2012, after an extreme drought which started in 2011, dieback and mortality events were observed in a Scots pine (*Pinus sylvestris* L.) population situated close to its southernmost distribution limit (Camarero et al. 2015a). The trees showing lower crown cover after the drought grew less since the 1980s (Camarero et al. 2015a) and showed smaller tracheid diameter than non-declining and less defoliated trees, but wider phloem sieve cells at the stem apex (Kiorapostolou et al. 2020; Pellizzari et al. 2016). Less than a decade after the extreme drought-triggered forest dieback, the Scots pine population has been decimated and more drought-tolerant species as junipers and oaks dominate the site (Gazol et al. 2018). The very high mortality rate (ca. 90–95% in some sites) has led to the near local extinction of the species, so understanding the dieback events is also of high socioeconomic interest.

Here we analyze the primary and secondary growth trends, needle dynamics, and the WUE_i in coexisting declining and non-declining Scots pine trees. We aim to answer these questions: Is there a significant relationship between climate and needle production in Mediterranean Scots pine populations? What climate factors are determining needle dynamics? Are there drought legacies in needle dynamics? Are past drops in needle production involved in radial growth decline, and thus accurate early-warning signals of dieback? We hypothesized that the annual production of needles is mainly related to a combination of previous year (year *n*-1) climate effects and the growing-season drought stress

(year n). Thus, sharp drops in needle production could reflect extensive xylem embolism in crown tissues in response to extreme droughts and indicate those trees more prone to subsequent droughts.

Materials and methods

Study site

This study took place in the forest called "El Carrascal", located in the municipality of Corbalán (Teruel province, northeastern Spain; 40° 26′ N, 0° 58′ W). It is a mixed forest formed by Scots pine, Black pine (*Pinus nigra* subsp. *salzmannii* (Dunal) Franco) and Portuguese oak (*Quercus faginea* Lam.), and other more thermophilic species dominating southern aspects such as Spanish juniper (*Juniperus thurifera* L.) or holm oak (*Quercus ilex* L.). The understory vegetation is formed by *Amelanchier ovalis* Medik. and *Arctostaphylos uva-ursi* (L.) Spreng. The forest basal area is 15 m^2 ha^{-1}. The main aspect is northwest, the slope is ca. 25° and the elevation is 1303 m a.s.l. The climate is continental Mediterranean with a mean annual temperature of 11.7 °C and the mean annual rainfall is 447 mm (Fig. S1). The forest was impacted by the 2011–2012 drought but also by previous droughts in 1985–1986, 1994–1995 and 2005 (Fig. S2). The soils are of cambisol type with a loamy texture and a mean pH of 7.7.

Primary and secondary growth and needle dynamics

During the spring of 2017, we selected five declining trees and five non-declining trees of similar diameter at breast height (dbh, measured at 1.3 m) and height (Table 1). We considered declining and non-declining trees those with a crown cover lower or higher than 50%, respectively (Camarero et al. 2015a; Sangüesa-Barreda et al. 2015). We did not consider age during the selection of the study trees.

To quantify the long-term dynamics of needle production in the stem axis, we used the so-called 'Needle Trace method' (Kurkela and Jalkanen 1990; Aalto and Jalkanen 1998). This method is very time-consuming but provides an accurate perspective of the apical needles' dynamics across time. Until now, this methodology has been mainly applied in boreal pine populations from northern Europe (e.g., Jalkanen et al. 1995; but see also Poljanšek et al. 2013, 2015). In this study, we developed some variations for trees showing very low growth rates as is the case of some Mediterranean, drought-prone Scots pine populations.

Pine species retain needles of different ages for several years. These needles leave a record (scar or trace) in the longitudinal section of the growth ring in which they

Table 1 Main characteristics and mean values of primary (PRI, stem length) and secondary growth (SEC, tree-ring width), needle production (NP) and annual needle number (ANN) for the selected trees before standardization for the study period (1975–2016)

	Non-declining	Declining
No. trees	5	5
Dbh (cm)*	20.8 ± 0.7	22.3 ± 1.3
Height (m)	10.0 ± 0.5	11.1 ± 0.7
Age (years)	$67 \pm 4a$	$130 \pm 5b$
Crown cover (%)	$96.0 \pm 2.4b$	$32.5 \pm 3.6a$
PRI (cm)	$8.4 \pm 0.9b$	$2.7 \pm 0.3a$
SEC (mm)	$1.1 \pm 0.1b$	$0.5 \pm 0.1a$
NP (No.)	$121 \pm 9b$	$60 \pm 5a$
ANN (No.)	$501 \pm 25b$	$220 \pm 17a$

Different letters show significant differences ($P < 0.05$) between declining and non-declining trees for each variable (Mann–Whitney test). Mean values $\pm$ standard errors

*Dbh: diameter at breast height

were formed (Fig. S3). The identification of these scars in dated tree rings along the apical axis makes it possible to quantify the number of apical needles produced annually throughout tree life. In this study, we focused on the 1975–2016 period which encompassed the recent shift toward drier conditions observed in the study area (Carnicer et al. 2019). First, the east orientation of each tree was marked (orientation in which the production of needles will be measured). The main stems of selected trees were cut in annual sections and transported to the laboratory. In a second phase, the annual longitudinal increments (here considered as measures of primary growth) were identified and cut by detecting the insertion of the branches that indicate their annual limits (Fig. S3a). The extreme of each of these sections were sanded and dated to determine the year to which it corresponds (Fritts 1976). To fulfill this task, tree rings were visually cross-dated and measured with a resolution of 0.001 mm using a semi-automatic LINTAB measuring device and the associated TSAP software (Rinntech, Heidelberg, Germany). The cross-dating process was evaluated using the COFECHA program (Holmes 1983). Once all the segments were dated, the length of each primary growth was measured, and the six innermost tree rings were marked. We selected six years because it is the maximum needle longevity that the Scots pine usually shows (see also Drenkhan et al. 2006; Poljanšek et al. 2015; Pouttu and Dobbertin 2000; Jankowski et al. 2017). In a third phase, each of the rings that harbor needle scars were delimited by marking the latewood with the help of a binocular magnifying glass (Fig. S3b). Afterward, the segments were longitudinally sanded until the scars of the needles were found in each tree ring/year. Scars were always counted in latewood, and

in a section marked at an angle of approximately 45° from the pith and in the east orientation (Figs. S3b and S3c; see Aalto and Jalkanen 1998). In very narrow rings (e.g., those formed between 1981 and 1986), very fine sandpaper was used to determine the exact limits with precision. Finally, two variables were calculated: (i) the needle production (NP), the number of needles in the main trunk in the year in question (originally called number of needles in Aalto and Jalkanen 1998); and (ii) the annual total number of needles (ANN), that is, the number of needles in the main trunk considering all shoots of different ages (see Aalto and Jalkanen 1998). In total, we reconstructed the needle dynamics through the assessment of 2460 longitudinal sections.

To remove the age-related and non-climatic signals (e.g., tree-to-tree competition), we detrended all analyzed series. Secondary (tree-ring width) and primary (stem length) series (abbreviated as SEC and PRI, respectively, hereafter), as well as NP and ANN series, were standardized applying a double detrending procedure. First, we fitted a negative exponential function followed by splines cut-off with a length equal to 2/3 length of series (Fritts 1976). Second, we applied autoregressive modeling to remove first-order temporal autocorrelation. This process is routinely done in dendrochronological studies to separate low- (mainly biological) and high-frequency (mainly climatic) variations. The standardized indexes of PRI, SEC, NP, and ANN time series were called PRI_i, SEC_i, NP_i, and ANN_i, respectively. This process was carried out using the *detrend* function in the R package *dplR* (Bunn et al. 2020; R Core Team 2020).

Climate data and drought index

To analyze the influence of climate on PRI, SEC, NP, and ANN, we used long-term (1975–2016) monthly climatic data (temperature, cloudiness, and water balance, i.e., the difference between precipitation and potential evapotranspiration or P-PET) from the Climate Research Unit (CRU) TS 4.01. database (Harris et al. 2020). This climatic repository provides homogenized and quality-controlled data at 0.5° spatial resolution. Climate time series were downloaded from the Climate Explorer of the Royal Netherlands Meteorological Institute (http://climexp.knmi.nl) for the grid in which the study site was located.

To analyze the impact of drought severity, we employed a multi-scalar drought index, the Standardized Precipitation Evapotranspiration Index (SPEI; Vicente-Serrano et al. 2010). We used 1–12-month SPEI timescales for the period 1975–2016 for the study site from a high-resolution gridded dataset available for Spain and based on quality-controlled and homogenized meteorological series (Vicente-Serrano et al. 2017).

Water-use efficiency

To compare the changes in WUE_i over time and between health categories, we measured the $^{13}C/^{12}C$ isotope ratio in wood during the 1975–2014 period. For this purpose, we extracted 5-mm tree cores at 1.3 m height that were cross-dated, and then the tree rings were individually separated with a razor blade with the help of a binocular microscope. Samples were grouped in 5-year segments (1975–79, 1980–1984, 1985–1989, 1990–1994, 1995–1999, 2000–2004, 2005–2009, and 2010–2014). We analyzed the same five declining trees and five non-declining trees that were used for the needle reconstruction. Wood samples were carefully homogenized and milled using an ultra-centrifugation mill (Retsch ZM1, mesh size of 0.5 mm). An aliquot of 0.6 mg of each wood sample was weighed on a balance (Mettler Toledo AX205) and placed into a tin capsule for isotopic analyses. The isotope ratio $^{13}C/^{12}C$ ($\delta^{13}C$) was determined on an isotope ratio mass spectrometer (Thermo Finnigan MAT 251) at the Stable Isotope Facility (Univ. California, Davis, CA, USA). The results were expressed as relative differences in the $^{13}C/^{12}C$ ratio of tree material with respect to the Vienna Pee-Dee Belemnite (V-PDB) standard. The estimated precision of the measurements was $\pm 0.1‰$.

Isotopic discrimination between the carbon of atmospheric CO_2 and plant carbon (Δ; see Farquhar and Richards 1984) was defined as:

$$\Delta = \left(\delta^{13}C_{atm} - \delta^{13}C_{plant}\right) \big/ \left(1 + \delta^{13}C_{plant}/1000\right), \quad (1)$$

where $\delta^{13}C_{atm}$ and $\delta^{13}C_{plant}$ are the isotope ratios of carbon ($^{13}C/^{12}C$) in atmospheric CO_2 and plant material, respectively, expressed in parts per thousand (‰) relative to the standard VPDB; Δ is linearly related to the ratio of intercellular (c_i) to atmospheric (c_a) CO_2 mole fractions, by (see Farquhar et al. 1982):

$$\Delta = a + (b - a)c_i/c_a, \quad (2)$$

where a is the fractionation during CO_2 diffusion through the stomata (4.4‰), and b is the fractionation associated with reactions by Rubisco and PEP carboxylase (27‰; Farquhar and Richards 1984). The c_i/c_a ratio reflects the balance between A and g_s. Thus, the linear relationship between c_i/c_a and Δ may be used to calculate WUE_i as follows:

$$WUE_i = (c_a/1.6)\left[(b - \Delta)/(b - a)\right] \quad (3)$$

Statistical analyses

First, we aimed to determine the influences of climate variables (temperature, precipitation, cloudiness, and P-PET) on PRI_i, SEC_i, NP_i, and ANN_i. Concretely, we run partial least squares (PLS) regressions for Generalized Linear Models (Gaussian family). This regression method predicts the values taken by the target variables from a series of predictor variables (temperature, precipitation, cloudiness, and water balance) using a multivariate approach. This approach sidesteps two difficulties, the collinearity of explanatory variables and the high number of variables. Climatic conditions were considered from year n-1 to year n, and we used 4 PLS components. We run independent models for each variable (PRI_i, SEC_i, NP_i, and ANN_i) including monthly, multi-month, and seasonal climate data. We grouped consecutive variables with a similar response in a stepwise process. Bootstrapping was carried out by generating 1000 replicates. In addition to PLS regressions, we related the individual time series and chronologies (i.e., averages of all individuals through years) of each variable with monthly climate data and the SPEI, using Pearson correlation coefficients. Climate–growth relationships were calculated from June of the year prior to tree-ring formation up to September of the year of tree-ring formation. We used the 1975–2016 period and monthly series of 1- to 12-month long SPEI.

Second, to assess potential differences in climate responses in declining and non-declining trees, we fitted linear mixed-effect models (LMMs; Pinheiro and Bates 2000) considering the standardized time series of PRI, SEC, NP, and ANN (PRI_i, TRW_i, NP_i, and ANN_i) as the dependent variables and climate variables as fixed factors. A separate model was fitted for each tree status (declining vs. non-declining) and variable (PRI, SEC, NP, and ANN) considering the period 1975–2016. First-order effects of January temperature for PRI, SEC, and NP, February temperature for SEC, and July temperature for ANN, and first- and second-order effects of annual P-PET were included. We included various water balance variables, such as June and September of the previous year for PRI and SEC, December of the previous year for NP and ANN, January for PRI and SEC, April for NP and ANN, June and July for ANN and SEC, and August for NP. We also included November cloudiness of the previous year for PRI, May for NP and ANN, and August and September for SEC. Finally, the interactions between crown cover and SPEI were also included (see Statistical Models in Supplementary Information). In the case of SPEI, we used the month and time scale with the highest correlation with PRI_i, TRW_i, NP_i, and ANN_i. We included year as crossed random factor of tree to incorporate the non-independent structure of our data. Climate variables were standardized to enable direct comparison of predictors'

coefficients. We calculated variance inflation factors (VIF) to assess collinearity among explanatory variables excluding second-order effects (Dormann et al. 2013). All variables showed VIF values lower than 3, suggesting no longer redundancy problems among predictors (Dormann et al. 2013; Zuur et al. 2009). Residuals normality and homoscedasticity were checked to confirm the assumptions of LMMs (Fig. S15). The strength of models was evaluated by calculating the marginal (proportion of variance explained by fixed factors) and conditional (variance explained by fixed and random factors) R^2 statistics as proposed by Nakagawa et al. (2017). We used the R package *plsRglm* (Bastien et al. 2005; Bertrand and Maumy-Bertrand 2018) to fit PLS regression models, *lme4* (Bates et al. 2015) to fit LMMs, *performance* (Lüdecke et al. 2020) to check collinearity, and *sjPlot* (Lüdecke et al. 2021) to visualize and calculate model statistics.

Lastly, we also determined the contribution of the annual needle production (NP) in the total annual number of needles (ANN). Thus, we calculated a variable called Canopy Completeness (CC), as follows:

$$CC = \log \left(\frac{NP}{ANN - NP} \right) \tag{4}$$

We used a log transformation to enhance the comparability between both vigor classes.

Drought legacies

Drought legacies or carryover effects in different meristems and carbon uptake organs (needles) might significantly affect dieback processes. We quantified the drought legacies in PRI, SEC, NP, and ANN applying a Bayesian hierarchical framework with the package *EcoMem* in R environment and using raw data (Itter et al. 2019, 2021). We included in all models the age of the trees in each year. We fitted all the models discriminating declining and non-declining trees. We defined a drought event those years with a drought index SPEI lower than − 1. We used the June SPEI calculated at a 5-month time scale (Camarero et al. 2015a). We evaluated the legacy effects for one to three years lags and considered 1000 Markov chain Monte Carlo simulations which were fitted to define 95% confidence interval (see Statistical Models in Supplementary Information).

Results

Growth and needle dynamics

The selected Scots pine individuals had significant differences in crown cover but also in age, with declining trees being older than non-declining trees (Table 1). The
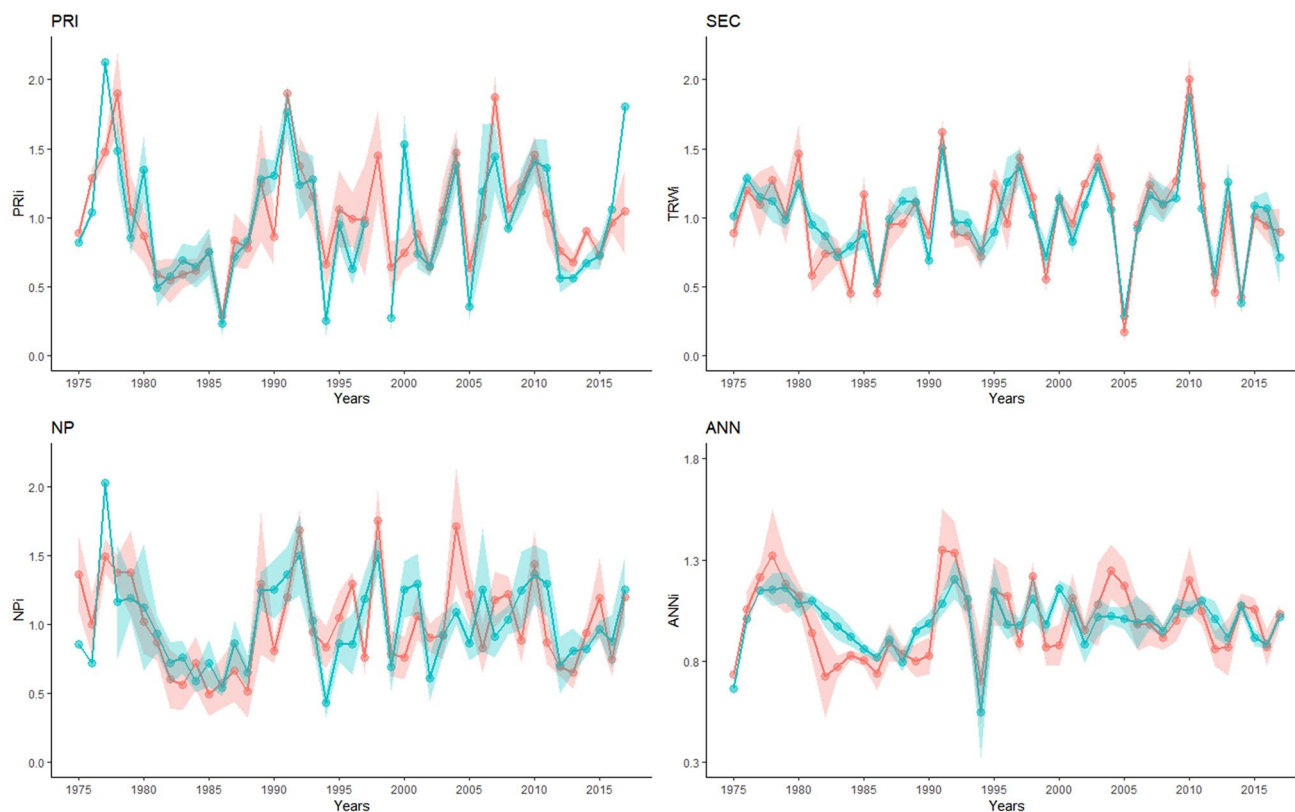
Fig. 1 Standardized values of primary (PRI) and secondary (SEC) growth, needle production (NP), and annual needle number (ANN) of declining (red) and non-declining (blue) trees. The red and blue areas show the standard errors

standardized series, after removing age-related signals, showed differences between vigor classes, particularly in the 1980s and considering ANN_i (Fig. 1). We detected sharp drops in needle production (NP_i and ANN_i) and stem length (PRI_i) in the dry 1986, 1994 and 2005 years, while tree-ring width (SEC_i) reductions were more important in the 2005 and 2012 droughts. Finally, the CC index indicated that the contribution of annual needle production to total crown cover was significantly higher in declining than non-declining trees in very dry periods (1980s, 1994–1995 or 2012; Fig. S4).

The Pearson correlations between site chronologies of PRI_i, SEC_i, NP_i, and ANN_i were high. SEC_i was positively and strongly correlated with PRI_i and NP_i ($r = 0.63$ and 0.40, respectively, df = 41, $P < 0.01$), but was not significant with ANN_i ($r = 0.25$). PRI_i was positively and significantly correlated with NP_i and ANN_i ($r = 0.75$ and 0.60, respectively, df = 41, $P < 0.001$). Finally, the correlation between NP_i and ANN_i was also positive and significant ($r = 0.72$, df = 41, $P < 0.001$).

Influence of climate on growth and needle dynamics

PRI was mainly enhanced by warm February and wet previous June (n-1) conditions (Figs. S5 and S6). Seasonally, PRI was enhanced by wet winters, warm springs, and cloudy previous autumns (n-1; Fig. S10). SEC was enhanced by wet and cloudy conditions during previous autumn (September) and winter (January; Figs. S5 and S7). Seasonally, SEC was enhanced by wet and cold winters (Fig. S11). On the other hand, wet conditions during previous winter (December) positively influenced NP and ANN (Figs. S5, S8, S9, S12, and S13). Wet conditions during April and previous November, and cold January temperatures negatively influenced NP. Finally, high temperatures in summer (July) also negatively influenced ANN.

Overall, declining trees responded more negatively to climate than non-declining trees (Fig. 2; Tables S1 and S2). For declining trees in PRI, NP, and ANN, spei (positive) were the most significant variables. Annual water balance had a negative effect on PRI, while June water balance of

the previous year had a positive effect. SEC was significantly influenced by the prior September (positive), January (positive), and July (negative) water balance. July temperatures had a negative effect in ANN while May cloudiness had a positive effect. The interaction of spei and crown cover was negative, especially in declining trees, although only significant in NP. No second-order effects of annual P-PET were detected for PRI, SEC, NP, and ANN.

The highest correlations between PRI and SEC with the SPEI were found at 9- to 10-month time scales in March and May, respectively (Fig. S14). The correlation was higher in the case of SEC ($r = 0.62$) than PRI ($r = 0.46$). On the contrary, the maximum correlation between NP and ANN with the SPEI was lower ($r = 0.36$) and occurred at short time scales (2–3 months) in January–February.

The dry 1980s showed the highest values of $\delta^{13}C$ since the 1970s, and similar WUE_i values to the 2000s (Fig. 3). Since the 2000s onwards, declining trees showed higher WUE_i than non-declining trees. Differences between health categories were only significant for the early 2000s and the late wet 1970s (Fig. 3). The 5-year WUE_i showed no significant correlations with PRI, SEC, NP, and ANN.

Drought legacies

We detected a higher variability of drought legacy effects in declining than in non-declining trees (Fig. 4), although PRI, SEC, and NP mean legacy values did not show strong differences in trees with different vigor. The most relevant drought legacies were found in ANN. Droughts had a significant legacy effect on ANN up to three years. In fact, posterior mean weight values greater than 0.2 were found for lags from 0 to 3 years, indicating persistent signals or carryover effects in needle production.

Discussion

Past severe droughts impaired needle production, canopy dynamics, and growth in this severely decimated Scots pine population. This information is supported by our field observations since recent extreme droughts also induced canopy dieback and tree death in this forest (Camarero et al. 2015a), where mortality increased at a rate of 0.22 y^{-1} in the period 2012–2017 reaching a value of 94% (Gazol et al. 2018). In this line, our results confirm the pervasive impact of droughts on leaf biomass because drought effects on crown cover were evident 3 years after drought occurrence. Our results also supported our hypothesis that needle development is driven by previous climate (year n-1) and growing-season water deficit (year n). We detected a long-term reduction in foliage along with a sharp increase in WUE_i in the warm-dry 1980s that probably triggered the dieback

episode (Figs. 1 and 3), although we cannot fully discard the contribution of defoliating insects such as the pine processionary moth (Sangüesa-Barreda et al. 2014). In line with the hypothesis that drought stress has an impact on crown condition, declining trees tended to show stronger drought legacy effects, particularly in the case of ANN, and were more negatively influenced by climate than non-declining trees (Figs. 2 and 4).

We acknowledge the limitation imposed by age differences between the tree health classes. We limited the potential impact of age by detrending the target variables. Nevertheless, declining trees were older than non-declining trees which could suggest a declining process related to ontogenic processes impairing hydraulic functioning during drought. However, this seems not to be the case, since extensive studies at this site have demonstrated that this dieback process was induced by extreme droughts and warming trends (Pellizzari et al. 2016; Camarero et al. 2015a), and that all mature trees, regardless of their age, were vulnerable to drought-induced dieback (cf. Camarero et al. 2015a). In line with this, Scots pine is able to reach hundreds of years old in nearby populations with no evidence of loss of vitality (Camarero et al. 2015b; Tejedor et al. 2017). Declining trees are, and were in the past, more vulnerable to climate. Such a long-term crown decline, even in younger trees, can be used to forecast their future growth and health trajectories (e.g., Dobbertin and Brang 2001).

Secondary growth was related to primary growth and needle production, indicating some overlapping signals to climate, particularly to soil water shortage. In fact, the secondary growth was enhanced by wet and cloudy conditions during previous autumn–winter and the current summer, which agrees with its strong responsiveness to drought stress compared with other remote-sensing proxies or indices of tree cover (Gazol et al. 2020). However, we did not find different legacies in secondary growth as a function of tree vigor, in contrast to ANN, which suggests that all trees could be chronically stressed considering stem wood production. This justifies measuring the annual total number of needles which allowed detecting more important legacy effects in declining than in non-declining pine trees.

A large body of research highlights the role of forcing temperatures in late winter to early spring on the onset of bud break during ecodormancy (Fløistad and Granhus 2010), and their positive effect on primary growth (Sutinen et al. 2012). These results are consistent with our findings as we found a prominent signal of February and March temperature on apical shoot growth (Fig. S6). We also found a negative effect of winter months (December and January) that could suggest that bud development during the last organogenesis phases was constrained by low temperatures, before bud bursting in spring. Water availability, and not temperature, drove needle production in this drought-stressed Scots pine population
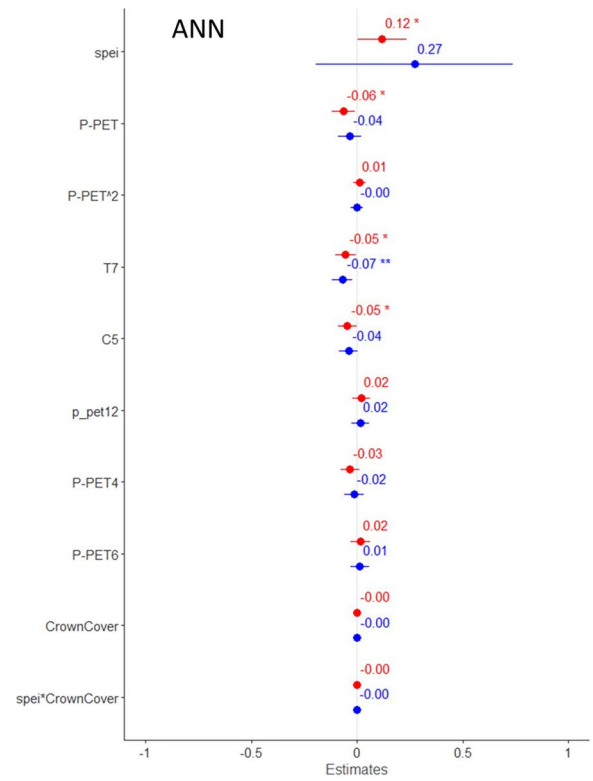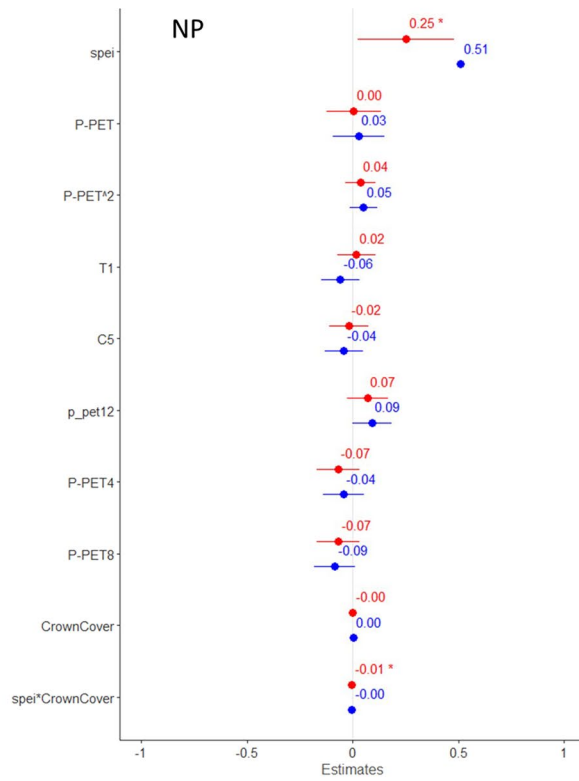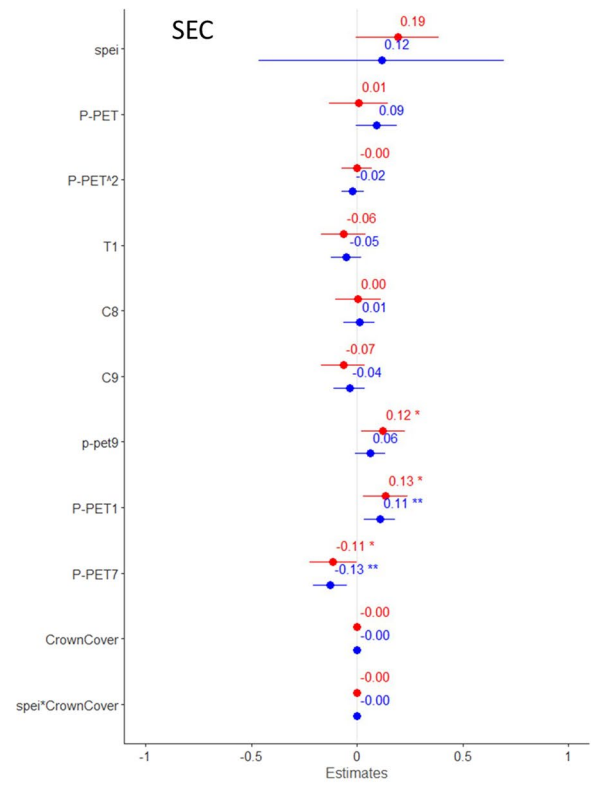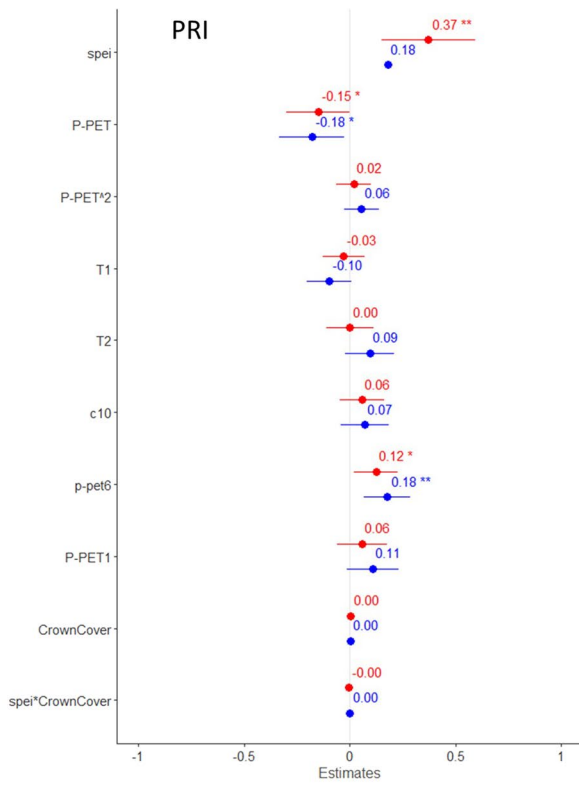
◄**Fig. 2** Linear mixed models output showing parameter estimates (standardized β values) as a function of primary (PRI) and secondary (SEC) growth, needle production (NP), and annual needle number (ANN) and climate variables of declining (red symbols) and non-declining (blue symbols) trees for the 1975–2016 period. Variables' abbreviations: standardized precipitation index (spei), annual water balance (P-PET), second-order effects of annual water balance (P-PET^2), January temperature (T1), February temperature (T2), July temperature (T7), November cloudiness of the year prior to tree-ring (c10), May cloudiness (C5), August cloudiness (C8), September cloudiness (C9), June water balance of the year prior (p-pet6), September water balance of the year prior (p-pet9), December water balance of the year prior (p-pet12), January water balance (P-PET1), April water balance (P-PET4), June water balance (P-PET6), July water balance (P-PET7), August water balance (P-PET8), and the interaction of spei and crown cover (spei*CrownCover). Thin lines represent the confidence intervals of standardized coefficients. Significance levels: ** = > 0.99 probability different from zero; * = > 0.95 probability

(Fig. 2; Figs. S5 and S8). In fact, winter water balance was positively correlated with needle abundance and production (Figs. S12 and S13), a positive effect maintained in December and January. Wet and snowy winters may recharge soil water reserves and positively influence needle development and tree growth in spring (Camarero et al. 2015a). This finding differs from other results on cold-limited Scots pine forests in northern Europe where needle longevity, leaf density, and leaf mass per area decreased as winter minimum temperature increased, but needle length increased (Pensa et al. 2010; Jankowski et al. 2017).

Regarding the negative effect of November water balance on needle production (Fig. S5), it is possible that drier and warmer conditions in the prior autumn led to a consumption of non-structural carbohydrates (NSCs) through enhanced respiration and reserve consumption (Martínez-Vilalta et al. 2016). This indirect effect would reduce needle growth in spring. In addition, these climate conditions could constrain bud growth and the development of preformed stem units which will transform into shoots and needles depending on temperature conditions (Schiestl-Aalto et al. 2013). In summer and autumn, stored NSCs may be also redirected to other carbon sinks such as seed maturation (McCartan et al. 2021). In line with our hypothesis, December and January water availability showed a positive signal on needle production, possibly enhancing bud development.

Needle abundance was negatively influenced by July temperature of the current year and the previous year (Fig. 2; Figs. S5 and S9), highlighting hotter drought as cause of premature needle thinning (Kurkela et al. 2009). Scots pine has isohydric behavior, i.e., it has a tight stomatal control of transpiration, avoiding hydraulic failure but limiting carbon assimilation (Klein 2014). If this situation continues in time, and trees reach a negative whole-plant C balance, metabolism must be sustained using stored NSC pools (Martín-Gómez et al. 2017). A depletion on NSCs might reach

tipping points and limit the ability of trees to recover from drought stress (McDowell et al. 2008). Our findings concur with Camarero et al. (2015a) who found a post drought reduction in the concentration of sapwood soluble sugars in severely defoliated, declining trees. Others (Poyatos et al. 2013; Salmon et al. 2015) also found that needles of defoliated trees had higher gas exchange rates and thus smaller hydraulic safety margins than in those from non-defoliated trees. This strategy would increase the risk of branch hydraulic failure and crown defoliation in declining trees.

Needle thinning mainly affects the less functional old needles with lower photosynthetic rates (Wang et al. 1995), and thus, in severe drought years, the new formed needles may represent a large part of the total foliage (Fig. S4). Such an abnormal turnover of foliage could indicate impending dieback in response to drought stress (Anfodillo et al. 2016). In addition, the canopy defoliation and the ability to form new needles and synthesize or mobilize NSCs may determine the recovery capacity of trees (Galiano et al. 2011). The drought-induced loss of the oldest needles produces changes in the crown that may last several years (Fig. 4; Fig. S4), and probably this legacy is one of the main causes of the delayed response of secondary growth to climate stress (Gazol et al. 2020). In this line, drops in needle production were observed in both declining and non-declining trees in dry periods, although it was especially dramatic the differences of needle abundance in the 1980s droughts (Fig. 1). The WUE$_i$ trends were consistent with those of needle abundance, and high values of WUE$_i$ were paired with needle drops, supporting the main role of drought in the reconstructed needle thinning. Our results contrasted with other studies that, using remote-sensing-based information, found non-significant drought stress impacts on forest primary production (Zhang et al. 2018) and agree with those studies that highlight declines in tree cover and leaf biomass as a major consequence of drought (Carnicer et al. 2011; Gazol and Camarero 2021). In this sense, Thabeet et al. (2009) found long-term defoliations and negative impacts on crown development in French Scots pine populations after consecutive severe droughts. Probably, the commented discrepancies depend on the scale of study since satellite images reflect cover and greenness at large scales, whereas our field measures better captured tree-to-tree variability and local responses to reduced soil water availability (Gazol et al. 2018).

The top shoot of a tree's bole is usually the most vigorous and has a high density of needles, but it may not be representative of the entire crown since high-hierarchical order branches receiving less radiation may not be represented despite accounting for most leaf area. Thus, it is essential to consider the top shoot and lateral branches given that crown transparency is influenced by active branch number and spatial distribution, which are affected by axes branching rate

Fig. 3 Carbon isotope ratios and intrinsic water-use efficiency (WUE$_i$) in declining (D) and non-declining (ND) trees. Different letters indicate significant ($p < 0.05$) differences between 5-year periods. Differences between health categories (D vs. ND) for each 5-year period were tested using one-way ANOVAs and are indicated with asterisks. Significance levels: *** = > 0.95 probability different from zero; ** = > 0.9 probability; * = > 0.85 probability
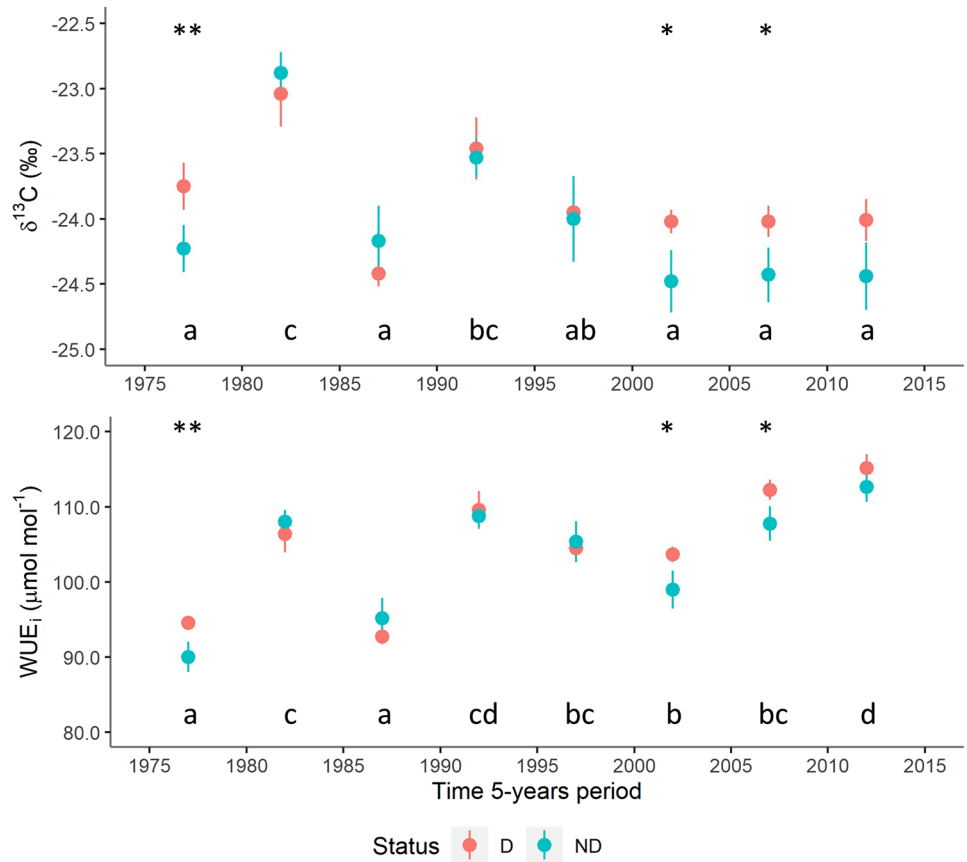
Fig. 4 Drought legacies on primary (PRI) and secondary (SEC) growth, needle production (NP) and annual needle production (ANN) in declining and non-declining trees. Black dots indicate the mean, and gray areas indicate 95% confidence interval
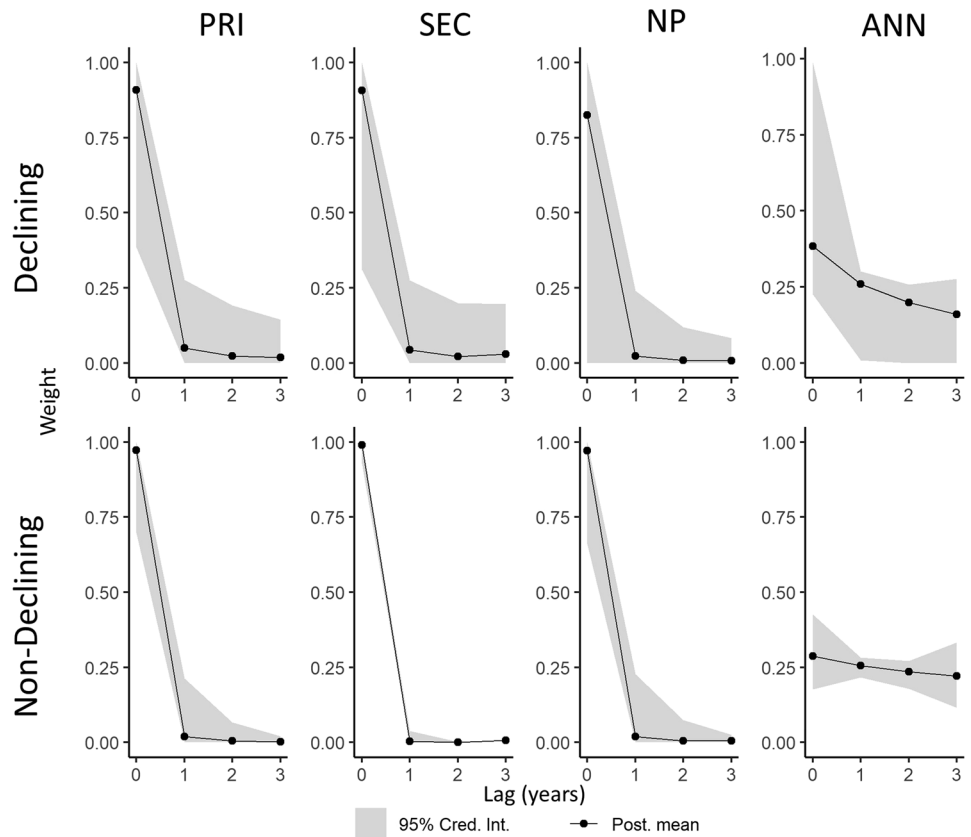
and branch death. Branching rate, needle number, and needle size all play critical roles in determining crown transparency (Thabeet et al. 2009). Drought, heat, and other stresses can lead to a reduction in active branch number, and slow recovery or event no recovery of branching rate which can limit needle number and leaf area, leading to tree decline and dieback (Vennetier et al. 2013).

In this study, we used WUE_i as an indicator of drought stress, but some considerations should be considered. On one hand, the link between tree ring $\delta^{13}C$ and WUE_i is not always straightforward. The non-negligible resistance to transport in the leaf mesophyll, particularly under stress, can affect photosynthetic discrimination (Cano et al. 2013). On the other hand, although it is out of the scope of this study, there can be some uncoupling between tree-ring isotopic signatures and leaf level physiological processes (e.g., Offermann et al. 2011). Finally, over long periods of time, the background CO_2-$\delta^{13}C$ can change, e.g., general atmospheric trend and possibly local changes due to sources of CO_2, which would affect the recorded $\delta^{13}C$ values even if the discrimination does not change.

Several of the considered droughts lasted more than one year (1985–1986, 1994–1995, 2011–2012), which could explain why we found stronger responses of PRI and SEC during some of these dry periods as compared to NP and ANN. We acknowledge that drought is not the only driver of growth in the study stand, where other climate extremes (heat and cold waves) or biotic factors (outbreaks) could have played a role, but it is a major stressor.

For many monocyclic conifers, including pines, preform needles in the previous year's (n-1) buds, this process determines the number of needles in the year n (Barthélémy and Caraglio 2007; Lanner 2017; Thabeet et al. 2009). While the climate of the current year (n) drives shoot elongation, the number of needles could show delayed responses. In this study, we consider different time scales, from monthly to seasonal, and from the previous year to the current year; however, we cannot fully discard multi-year delayed responses. In addition, declining trees with reduced diameter growth could exhibit a longer average needle lifespan than non-declining trees with higher diameter growth. For example, Pensa and Sellin (2002) observed a significant negative correlation between shoot length increment and needle lifespan for Scots pine. However, it is important to note that an accurate retrospective tracking of needle lifespan is not feasible.

The search for reliable early-warning signals of dieback at multiple spatial and temporal scales has been a constant in the last years (e.g., Camarero et al. 2015a). The temporal features of radial growth series have been largely used, such as lower growth rates (Cailleret et al. 2017), increased climatic sensitivity (Ogle et al. 2000), increased persistence or autocorrelation, and decreased synchrony or tree-to-tree

coherence in growth (Camarero et al. 2015a; Cailleret et al. 2019), or lower resistance and resilience to drought (DeSoto et al. 2020). However, this information is incomplete due to the long mismatch between climate drivers and growth responses and the lack of information regarding foliage dynamics. Our results indicate that the reconstruction of past needle abundance trends is a reliable early-warning signal of dieback. Trees with severe previous crown defoliations may be more vulnerable to subsequent droughts, as indicated by more severe defoliations in the 1980s in currently defoliated trees. Other physiological measures of tree vigor such as the relative water content of tissues (Martinez-Vilalta et al. 2019) have been proposed, but in those cases, long-term temporal series are lacking. We acknowledge the challenges associated with reconstructing needle abundance over time, including the potential time and cost constraints, as well as the destructive nature of the Needle Trace method. However, needle persistence on annual shoots is easily visible with binoculars in pine species, and it could serve as a useful first indicator of tree crown transparency. Nevertheless, our study suggests a promising new direction for future research utilizing remote-sensing techniques or drones with rapidly improving spatial and temporal resolution. These advances in technology could offer a non-destructive alternative, facilitating a better understanding of long-term trends in forest health. Remote sensing is useful to monitor tree and forest leaf area across large spatial scales, but detailed field studies are needed to validate remote-sensing data, and to accurately assess the complex needle dynamics at tree and branch scales and how they relate to primary and secondary growth.

At population level, some trees have an extraordinary capacity to adjust to their environmental conditions showing different responses to drought stress such as growth plasticity. Here we show that trees with a higher needle thinning after drought had a higher probability to suffer dieback. Our results indicate that: (i) reconstructions of needle production contain reliable early-warning signals of drought-induced dieback, (ii) and long-term canopy dynamics should be further explored to forecast changes in tree health.

Conclusions

We detected drought-induced drops in needle production decades before extensive forest dieback concurring with divergent growth trends between declining and healthy trees. Thus, we interpreted these changes in the crown as a major cause of the long-term forest dieback process. Trees decimated by sudden drops in needle abundance would show lower hydraulic conductivity, extensive xylem embolism and reduced pools of NSCs and stored tissue water. In addition, the progressive loss of photosynthetic tissues limits carbon uptake increasing the risk of carbon starvation and

accelerating the dieback process. Our results support past needle drops as early-warning signals of drought-induced dieback in Scots pine.

Data availability The data are available upon a reasonable request to the Authors.

Declarations

Conflict of interest The authors declare that they have no conflict of interest.

References

Aalto T, Jalkanen R (1998) Neulasjälkimenetelmä. The needle trace method. Metsäntutkimuslaitoksen tiedonantoja—research Papers 681. p 36. ISBN 951-40-1619-X

Adams HD, Zeppel MJB, Anderegg WRL, Hartmann H, Landhäusser SM, Tissue DT, Huxman TE, Hudson PJ, Franz TE, Allen CD, Anderegg LDL, Barron-Gafford GA, Beerling DJ, Breshears DD, Brodribb TJ, Bugmann H, Cobb RC, Collins AD, Dickman LT, Duan H, Ewers BE, Galiano L, Galvez DA, Garcia-Forner N, Gaylord ML, Germino MJ, Gessler A, Hacke UG, Hakamada R, Hector A, Jenkins MW, Kane JM, Kolb TE, Law DJ, Lewis JD, Limousin JM, Love DM, Macalady AK, Martínez-Vilalta J, Mencuccini M, Mitchell PJ, Muss JD, O'Brien MJ, O'Grady AP, Pangle RE, Pinkard EA, Piper FI, Plaut JA, Pockman WT, Quirk J, Reinhardt K, Ripullone F, Ryan MG, Sala A, Sevanto S, Sperry JS, Vargas R, Vennetier M, Way DA, Xu C, Yepez EA, McDowell NG (2017) A multi-species synthesis of physiological mechanisms in drought-induced tree mortality. Nat Ecol Evol 1:1285–1291. https://doi.org/10.1038/s41559-017-0248-x

Allen CD, Breshears DD, Mcdowell NG (2015) On underestimation of global vulnerability to tree mortality and forest die-off from hotter drought in the Anthropocene. Ecosphere 6:1–55. https://doi.org/10.1016/j.foreco.2009.09.001

Anfodillo T, Petit G, Sterck F, Lechthaler S, Olson ME (2016) Allometric trajectories and "stress": a quantitative approach. Front Plant Sci. https://doi.org/10.3389/fpls.2016.01681

Barthélémy D, Caraglio Y (2007) Plant architecture: a dynamic, multilevel and comprehensive approach to plant form, structure and ontogeny. Ann Bot 99:375–407. https://doi.org/10.1093/aob/mcl260

Bastien P, Vinzi VE, Tenenhaus M (2005) PLS generalised linear regression. Comput Stat Data Anal Partial Least Squares 48:17–46. https://doi.org/10.1016/j.csda.2004.02.005

Bates D, Mächler M, Bolker B, Walker S (2015) Fitting linear mixed-effects models using lme4. J Stat Softw 67:51. https://doi.org/10.18637/jss.v067.i01

Batllori E, Lloret F, Aakala T, Anderegg WRL, Aynekulu E (2020) Forest and woodland replacement patterns following drought-related mortality. PNAS 117:29720–29729. https://doi.org/10.1073/pnas.2002314117

Bertrand F, Maumy-Bertrand M (2018) plsRglm: partial least squares linear and generalized linear regression for processing incomplete datasets by cross-validation and bootstrap techniques with R. Preprint at arXiv:1810.01005 (Stat)

Bréda N, Huc R, Granier A, Dreyer E (2006) Temperate forest trees and stands under severe drought: a review of ecophysiological responses, adaptation processes and long-term consequences. Ann For Sci 63:625–644. https://doi.org/10.1051/forest:2006042

Bunn A, Korpela M, Biondi F, Campelo F, Mérian P, Qeadan F, Zang C (2020) dplR: dendrochronology program library in R. R Package Version 1(7):1

Cabon A, Fernández-de-Uña L, Gea-Izquierdo G, Meinzer FC, Woodruff DR, Martínez-Vilalta J, De Cáceres M (2020) Water potential control of turgor-driven tracheid enlargement in Scots pine at its xeric distribution edge. New Phytol 225:209–221. https://doi.org/10.1111/nph.16146

Cailleret M, Jansen S, Robert EMR, Desoto L, Aakala T, Antos JA, Beikircher B, Bigler C, Bugmann H, Caccianiga M, Čada V, Camarero JJ, Cherubini P, Cochard H, Coyea MR, Čufar K, Das AJ, Davi H, Delzon S, Dorman M, Gea-Izquierdo G, Gillner S, Haavik LJ, Hartmann H, Hereş AM, Hultine KR, Janda P, Kane JM, Kharuk VI, Kitzberger T, Klein T, Kramer K, Lens F, Levanic T, Linares JC, Lloret F, Lobo-Do-Vale R, Lombardi F, López Rodríguez R, Mäkinen H, Mayr S, Mészáros I, Metsaranta JM, Minunno F, Oberhuber W, Papadopoulos A, Peltoniemi M, Petritan AM, Rohner B, Sangüesa-Barreda G, Sarris D, Smith JM, Stan AB, Sterck F, Stojanović DB, Suarez ML, Svoboda M, Tognetti R, Torres-Ruiz JM, Trotsiuk V, Villalba R, Vodde F, Westwood AR, Wyckoff PH, Zafirov N, Martínez-Vilalta J (2017) A synthesis of radial growth patterns preceding tree mortality. Glob Chang Biol 23:1675–1690. https://doi.org/10.1111/gcb.13535

Cailleret M, Dakos V, Jansen S, Robert EMR, Aakala T, Amorso MM, Antos JA, Bigler C, Bugmann H, Caccianaga M, Camarero J-J, Cherubini P, Coyea MR, Čufar K, Das AJ, Davi H, Gea-Izquierdo G, Gillner S, Haavik LJ, Hartmann H, Hereş A-M, Hultine KR, Janda P, Kane JM, Kharuk VI, Kitzberger T, Klein T, Levanic T, Linares J-C, Lombardi F, Mäkinen H, Mészáros I, Metsaranta JM, Oberhuber W, Papadopoulos A, Petritan AM, Rohner B, Sangüesa-Barreda G, Smith JM, Stan AB, Stojanovic DB, Suarez M-L, Svoboda M, Trotsiuk V, Villalba R, Westwood AR, Wyckoff PH, Martínez-Vilalta J (2019) Early-warning signals of individual tree mortality based on annual radial growth. Front Plant Sci 8:1964. https://doi.org/10.3389/fpls.2018.01964

Camarero JJ, Gazol A, Sangüesa-Barreda G, Oliva J, Vicente-Serrano SM (2015a) To die or not to die: early-warning signals of dieback in response to a severe drought. J Ecol 103:44–57. https://doi.org/10.1111/1365-2745.12295

Camarero JJ, Gazol A, Tardif JC, Conciatori F (2015b) Attributing forest responses to global-change drivers: limited evidence of a CO_2-fertilization effect in Iberian pine growth. J Biogeogr 42:2220–2233. https://doi.org/10.1111/jbi.12590

Cano FJ, Sánchez-Gómez D, Rodríguez-Calcerrada J, Warren CR, Gil L, Aranda I (2013) Effects of drought on mesophyll conductance and photosynthetic limitations at different tree canopy layers. Plant Cell Environ 36:1961–1980. https://doi.org/10.1111/pce.12103

Carnicer J, Coll M, Ninyerola M, Pons X, Sánchez G, Peñuelas J (2011) Widespread crown condition decline, food web disruption, and amplified tree mortality with increased climate change-type drought. Proc Natl Acad Sci USA 108:1474–1478. https://doi.org/10.1073/pnas.1010070108

Carnicer J, Domingo-Marimon C, Ninyerola M, Camarero JJ, Bastos A, López-Parages J, Rodríguez-Fonseca B, Lenton TM, Dakos V, Ribas M, Gutiérrez E, Peñuelas J, Pons X (2019) Regime shifts of Mediterranean forest carbon uptake and reduced resilience driven by multidecadal ocean surface temperature. Global Change Biol 25:2825–2840. https://doi.org/10.1111/gcb.14664

Dai A (2013) Increasing drought under global warming in observations and models. Nat Clim Chang 3:52–58. https://doi.org/10.1038/NCLIMATE1633

DeSoto L, Cailleret M, Sterck F, Jansen S, Kramer K, Robert E, Aakala T, Amoroso M, Bigler C, Camarero JJ, Cufar K, Gea-Izquierdo G, Gillner S, Haavik L, Heres A-M, Kane J, Kharuk V, Kitzberger T, Klein T, Levanic T, Linares JC, Makinen H, Oberhuber W, Papadopoulos A, Rohner B, Sangüesa-Barreda G, Stojanovic D, Suarez LM, Villalba R, Martinez-Vilalta J (2020) Low growth resilience to drought is related to future mortality risk in trees. Nat Comm 11:545. https://doi.org/10.1038/s41467-020-14300-5

Dormann CF, Elith J, Bacher S, Buchmann C, Carl G, Carré G, García Marquéz JR, Gruber B, Lafourcade B, Leitão PJ, Münkemüller T, McClean C, Osborne PE, Reineking B, Chröder B, Skidmore AK, Zurell D, Lautenbach S (2013) Collinearity: a review of methods to deal with it and a simulation study evaluating their performance. Ecography 36:27–46. https://doi.org/10.1111/j.1600-0587.2012.07348.x

Drenkhan R, Kurkela T, Hanso M (2006) The relationship between the needle age and the growth rate in Scots pine (*Pinus sylvestris*): a retrospective analysis by needle trace method (NTM). Eur J For Res 125:397–405. https://doi.org/10.1007/s10342-006-0131-9

Fang J, Lutz JA, Shugart H, Yan X (2020) A physiological model for predicting dynamics of tree stem-wood nonstructural carbohydrates. J Ecol 108:702–718. https://doi.org/10.1111/1365-2745.13274

Farquhar GD, Richards R (1984) Isotopic composition of plant carbon correlates with water-use efficiency of wheat genotypes. Funct Plant Biol 11:539–552. https://doi.org/10.1071/PP9840539

Farquhar GD, O'Leary MH, Berry JA (1982) On the relationship between carbon isotope discrimination and the intercellular carbon dioxide concentration in leaves. Austral J Plant Physiol 9:121–137

Fløistad IS, Granhus A (2010) Bud break and spring frost hardiness in *Picea abies* seedlings in response to photoperiod and temperature treatments. Can J For Res 40:968–976. https://doi.org/10.1139/X10-050

Fritts HC (1976) Tree Rings and Climate. Academic Press, London

Galiano L, Martínez-Vilalta J, Lloret F (2011) Carbon reserves and canopy defoliation determine the recovery of Scots pine 4 yr after a drought episode. New Phytol 190:750–759. https://doi.org/10.1111/j.1469-8137.2010.03628.x

Gazol A, Camarero JJ (2021) Compound climate events increase tree drought mortality across European forests. Sci Tot Environ 816:151604. https://doi.org/10.1016/j.scitotenv.2021.151604

Gazol A, Camarero JJ, Sangüesa-Barreda G, Vicente-Serrano SM (2018) Post-drought resilience after forest die-off: shifts in regeneration, composition, growth and productivity. Front Plant Sci 9:1546. https://doi.org/10.3389/fpls.2018.01546

Gazol A, Camarero JJ, Sánchez-Salguero R, Vicente-Serrano SM, Serra-Maluquer X, Gutiérrez E, De Luis M, Sangüesa-Barreda G, Novak K, Rozas V, Tíscar PA, Linares JC, Martínez del Castillo E, Ribas M, García-González I, Silla F, Camisón A, Génova M, Olano JM, Hereş A-M, Curiel Yuste J, Longares LA, Hevia A, Tomàs-Burguera M, Galván JD (2020) Drought legacies are short, prevail in dry conifer forests and depend on growth variability. J Ecol 6:2473–2484. https://doi.org/10.1111/1365-2745.13435

Harris I, Osborn TJ, Jones P, Lister D (2020) Version 4 of the CRU TS monthly high-resolution gridded multivariate climate dataset. Sci Data 7:109. https://doi.org/10.6084/m9.figshare.11980500

Hartmann H, Bastos A, Das AJ, Esquivel-Muelbert A, Hammond WM, Martínez-Vilalta J, McDowell NG, Powers JS, Pugh TAM, Ruthrof KX, Allen CD (2022) Climate change risks to global forest health: emergence of unexpected events of elevated tree mortality worldwide. Annu Rev Plant Biol. https://doi.org/10.1146/annurev-arplant-102820-012804

Holmes RL (1983) Computer-assisted quality control in tree-ring dating and measurement. Tree-Ring Bull 43:69–78

Itter MS, Vanhatalo J, Finley AO (2019) EcoMem: an R package for quantifying ecological memory. Environ Model Soft 119:305–308. https://doi.org/10.1016/j.envsoft.2019.06.004

Itter M, Vanhatalo J, Finley A (2021) EcoMem: Functions to Estimate Ecological Memory (R package version 0.0.0.9000). Environ Model Softw. https://doi.org/10.1016/j.envsoft.2019.06.004

Jalkanen R, Aalto T, Kurkela T (1995) Development of needle retention in Scots pine (*Pinus sylvestris*) in 1957–1991 in northern and southern Finland. Trees 10:125–133. https://doi.org/10.1007/BF00192193

Jankowski A, Wyka TP, Żytkowiak R, Nihlgard B, Reich PB, Oleksyn J (2017) Cold adaptation drives variability in needle structure and anatomy in *Pinus sylvestris* L. along a 1,900 km temperate–boreal transect. Funct Ecol 31:2212–2223. https://doi.org/10.1111/1365-2435.12946

Kannenberg SA, Novick KA, Alexander MR, Maxwell JT, Moore DJ, Phillips RP et al (2019) Linking drought legacy effects across scales: from leaves to tree rings to ecosystems. Global Change Biol 25:2978–2992. https://doi.org/10.1111/gcb.14710

Kiorapostolou N, Camarero JJ, Carrer M, Sterck F, Brigita B, Sangüesa-Barreda G, Petit G (2020) Scots pine trees react to drought by increasing xylem and phloem conductivities. Tree Physiol 40:774–781. https://doi.org/10.1093/treephys/tpaa033

Klein T (2014) The variability of stomatal sensitivity to leaf water potential across tree species indicates a continuum between

isohydric and anisohydric behaviours. Funct Ecol 28:1313–1320. https://doi.org/10.1111/1365-2435.12289

Kurkela T, Jalkanen R (1990) Revealing past needle retention in *Pinus* spp. Scand J For Res 5:481–485. https://doi.org/10.1080/02827589009382630

Kurkela T, Drenkhan R, Vuorinen M, Hanso M (2009) Growth response of young Scots pines to needle loss assessed from productive foliage. For Stud 50:5–22. ISSN 1406-9954

Lanner RM (2017) Primordium initiation drives tree growth. Ann For Sci 74:1–7. https://doi.org/10.1007/s13595-016-0612-z

López R, Javier Cano F, Rodríguez-Calcerrada J, Sangüesa-Barreda G, Gazol A, Camarero JJ, Rozenberg P, Gil L (2021) Tree-ring density and carbon isotope composition are early-warning signals of drought-induced mortality in the drought tolerant Canary Island pine. Agric For Meteorol 310:108634. https://doi.org/10.1016/j.agrformet.2021.108634

Lüdecke D, Makowski D, Waggoner P, Patil I (2020) Assessment of Regression Models Performance. CRAN

Lüdecke D, Bartel A, Schwemmer C, Powell C, Djalovski A, Titz J (2021) sjPlot: Data Visualization for Statistics in Social Science. R package version 2.8.10.2. https://CRAN.R-project.org/package=sjPlot

Martínez-Vilalta J (2018) The rear window: structural and functional plasticity in tree responses to climate change inferred from growth rings. Tree Physiol 38:155–158. https://doi.org/10.1093/treephys/tpy008

Martínez-Vilalta J, Sala A, Asensio D, Galiano L, Hoch G, Palacio S, Piper FI, Lloret F (2016) Dynamics of non-structural carbohydrates in terrestrial plants: a global synthesis. Ecol Monogr 86:495–516. https://doi.org/10.1002/ecm.1231

Martinez-Vilalta J, Anderegg WRL, Sapes G, Sala A (2019) Greater focus on water pools may improve our ability to understand and anticipate drought-induced mortality in plants. New Phytol 223:22–32. https://doi.org/10.1111/nph.15644

Martín-Gómez P, Aguilera M, Pemán J, Gil-Pelegrín E, Ferrio JP (2017) Contrasting ecophysiological strategies related to drought: the case of a mixed stand of Scots pine (*Pinus sylvestris*) and a submediterranean oak (*Quercus subpyrenaica*). Tree Physiol 37:1478–1492. https://doi.org/10.1093/treephys/tpx101

Martin-StPaul N, Delzon S, Cochard H (2017) Plant resistance to drought depends on timely stomatal closure. Ecol Lett 20:1437–1447. https://doi.org/10.1111/ele.12851

McCartan SA, Forster J, Jinks RL, Rampart MP, Cahalan CM (2021) The effect of temperature during cone and seed development on primary dormancy of Scots pine (*Pinus sylvestris* L.) seeds. New For. https://doi.org/10.1007/s11056-021-09884-9

McDowell NG, Pockman WT, Allen CD, Breshears DD, Cobb N, Kolb T, Plaut J, Sperry J, West A, Williams DG, Yepez EA (2008) Mechanisms of plant survival and mortality during drought: why do some plants survive while others succumb to drought? New Phytol 178:719–739. https://doi.org/10.1111/j.1469-8137.2008.02436.x

McDowell NG, Beerling DJ, Breshears DD, Fisher RA, Raffa KF, Stitt M (2011) The interdependence of mechanisms underlying climate-driven vegetation mortality. Trends Ecol Evol 26:523–532. https://doi.org/10.1016/j.tree.2011.06.003

McDowell NG, Sapes G, Pivovaroff A, Adams HD, Allen CD, Anderegg WRL, Arend M, Breshears DD, Brodribb T, Choat B, Cochard H, De Cáceres M, De Kauwe MG, Grossiord C, Hammond WM, Hartmann H, Hoch G, Kahmen A, Klein T, Mackay DS, Mantova M, Martínez-Vilalta J, Medlyn BE, Mencuccini M, Nardini A, Oliveira RS, Sala A, Tissue DT, Torres-Ruiz JM, Trowbridge AM, Trugman AT, Wiley E, Xu C (2022) Mechanisms of woody-plant mortality under rising drought, CO_2 and vapour pressure deficit. Nat Rev Earth Environ 0123456789:41–44. https://doi.org/10.1038/nature01096

Michelot A, Simard S, Rathgeber C, Dufrêne E, Damesin C (2012) Comparing the intra-annual wood formation of three European species (*Fagus sylvatica*, *Quercus petraea* and *Pinus sylvestris*) as related to leaf phenology and non-structural carbohydrate dynamics. Tree Physiol 32:1033–1045. https://doi.org/10.1093/treephys/tps052

Nakagawa S, Johnson PCD, Schielzeth H (2017) The coefficient of determination R2 and intra-class correlation coefficient from generalized linear mixed-effects models revisited and expanded. J Royal Soc Interf 14:213. https://doi.org/10.1098/rsif.2017.0213

Offermann C, Ferrio JP, Holst J, Grote R, Siegwolf R, Kayler Z, Gessler A (2011) The long way down—are carbon and oxygen isotope signals in the tree ring uncoupled from canopy physiological processes? Tree Physiol 31:1088–1102. https://doi.org/10.1093/treephys/tpr093

Ogle K, Whitham TG, Cobb NS (2000) Tree-ring variation in pinyon predicts likelihood of death following severe drought. Ecology 81:3237–3243. https://doi.org/10.1890/0012-9658(2000)081[3237:TRVIPP]2.0.CO;2

Pellizzari E, Camarero JJ, Gazol A, Sangüesa-Barreda G, Carrer M (2016) Wood anatomy and carbon-isotope discrimination support long-term hydraulic deterioration as a major cause of drought-induced dieback. Global Change Biol 22:2125–2137. https://doi.org/10.1111/gcb.13227

Pensa M, Jalkanen R (2005) Variation in needle longevity is related to needle-fascicle production rate in *Pinus sylvestris*. Tree Physiol 25:1265–1271. https://doi.org/10.1093/treephys/25.10.1265

Pensa M, Sellin A (2002) Needle longevity of Scots pine in relation to foliar nitrogen content, specific leaf area, and shoot growth in different forest types. Can J For Res 32:1225–1231. https://doi.org/10.1139/x02-044

Pensa M, Karu H, Luud A, Kund K (2010) Within-species correlations in leaf traits of three boreal plant species along a latitudinal plant gradient. Plant Ecol 208:155–166. https://doi.org/10.1007/s11258-009-9695-z

Pinheiro JC, Bates DM (2000) Mixed-effects models in S and S-PLUS. Springer, New York

Pinheiro C, Chaves MM (2011) Photosynthesis and drought: can we make metabolic connections from available data? J Exp Bot 62:869–882. https://doi.org/10.1093/jxb/erq340

Poljanšek S, Ballian D, Jalkanen R, Levanič T (2013) Evidence of massive growth decline in *Pinus nigra* trees using the needle trace method. In: Tree rings in archeology, climatology and ecology—TRACE 2013: program and abstracts of the dendrosymposium, Viterbo, p 97

Poljanšek S, Levanič T, Ballian D, Jalkanen R (2015) Tree growth and needle dynamics of *P. nigra* and *P. sylvestris* and their response to climate and fire disturbances. Trees 29:683–694. https://doi.org/10.1007/s00468-014-1146-3

Pouttu A, Dobbertin M (2000) Needle-retention and density patterns in *Pinus sylvestris* in the Rhone Valley of Switzerland: comparing results of the needle-trace method with visual defoliation assessments. Can J For Res 30:1973–1982. https://doi.org/10.1139/x00-127

Poyatos R, Aguadé D, Galiano L, Mencuccini M, Martínez-Vilalta J (2013) Drought-induced defoliation and long periods of near-zero gas exchange play a key role in accentuating metabolic decline of Scots pine. New Phytol 200:388–401. https://doi.org/10.1111/nph.12278

R Core Team (2020) R: a language and environment for statistical computing. R foundation for statistical computing

Rossi S, Deslauriers A, Griçar J, Seo JW, Rathgeber CBK, Anfodillo T, Morin H, Levanic T, Oven P, Jalkanen R (2008) Critical

temperatures for xylogenesis in conifers of cold climates. Glob Ecol Biogeogr 17:696–707. https://doi.org/10.1111/j.1466-8238.2008.00417.x

Salmon Y, Torres-Ruiz JM, Poyatos R, Martinez-Vilalta J, Meir P, Cochard H, Mencuccini M (2015) Balancing the risks of hydraulic failure and carbon starvation: a twig scale analysis in declining Scots pine. Plant Cell Environ 38:2575–2588. https://doi.org/10.1111/pce.12572

Sangüesa-Barreda G, Camarero JJ, García-Martín A, Hernández R, de la Riva J (2014) Remote-sensing and tree-ring based characterization of forest defoliation and growth loss due to the Mediterranean pine processionary moth. For Ecol Manag 320:171–181. https://doi.org/10.1016/j.foreco.2014.03.008

Sangüesa-Barreda G, Camarero JJ, Oliva J, Montes F, Gazol A (2015) Past logging, drought and pathogens interact and contribute to forest dieback. Agric For Meteorol 208:85–94. https://doi.org/10.1016/j.agrformet.2015.04.011

Saurer M, Spahni R, Frank DC, Joos F, Leuenberger M, Loader NJ, McCarroll D, Gagen M, Poulter B, Siegwolf RT, Andreu-Hayles L, Boettger T, Dorado Liñan I, Fairchild IJ, Friedrich M, Gutierrez E, Haupt M, Hilasvuori E, Heinrich I, Helle G, Grudd H, Jalkanen R, Levanic T, Linderholm HW, Robertson I, Sonninen E, Treydte K, Waterhouse JS, Woodley EJ, Wynn PM, Young GH (2014) Spatial variability and temporal trends in water-use efficiency of European forests. Global Change Biol 20:2109–2120. https://doi.org/10.1111/gcb.12717

Schiestl-Aalto P, Nikinmaa E, Mäkelä A (2013) Duration of shoot elongation in Scots pine varies within crown and between years. Ann Bot 112:1181–1191. https://doi.org/10.1093/aob/mct180

Sutinen S, Partanen J, Viherä-Aarnio A, Häkkinen R (2012) Development and growth of primordial shoots in Norway spruce buds before visible bud burst in relation to time and temperature in the field. Tree Physiol 32:87–997. https://doi.org/10.1093/treephys/tps063

Tejedor E, Saz MA, Esper J, Cuadrat JM, de Luis M (2017) Summer drought reconstruction in northeastern Spain inferred from a tree ring latewood network since 1734. Geophys Res Lett 44:8492–8500. https://doi.org/10.1002/2017GL074748

Thabeet A, Vennetier M, Gadbin-Henry C, Denelle N, Roux M, Caraglio Y, Vila B (2009) Response of *Pinus sylvestris* L. to recent climatic events in the French Mediterranean region. Trees 23:843–853. https://doi.org/10.1007/s00468-009-0326-z

Trugman AT, Anderegg LDL, Anderegg WRL, Das AJ, Stephenson NL (2021) Why is tree drought mortality so hard to predict? Trends Ecol Evol 36:520–532. https://doi.org/10.1016/j.tree.2021.02.001

Vennetier M, Girard F, Taugourdeau O, Cailleret M, Caraglio Y, Sabatier SA, Ouarmim S, Didier C, Thabeet A (2013) Climate change impact on tree architectural development and leaf area. Climate change: Realities, impacts over ice cap, sea level and risks. B. R. Singh. Rijeka, InTech, pp 103–126. https://doi.org/10.5772/51510

Vicente-Serrano SM, Beguería S, López-Moreno JI (2010) A multiscalar drought index sensitive to global warming: the standardized precipitation evapotranspiration index. J Clim 23:1696–1718. https://doi.org/10.1175/2009JCLI2909.1

Vicente-Serrano SM, Tomas-Burguera M, Beguería S et al (2017) A high resolution dataset of drought indices for Spain. Data 2:22. https://doi.org/10.3390/data2030022

Wang K-Y, Kellomäki S, Laitinen K (1995) Effects of needle age, long-term temperature and CO_2 treatments on the photosynthesis of Scots pine. Tree Physiol 15:211–218. https://doi.org/10.1093/treephys/15.4.211

Wang W, Peng C, Kneeshaw DD, Larocque GR, Luo Z (2012) Drought-induced tree mortality: ecological consequences, causes, and modeling. Environ Rev 20:109–121. https://doi.org/10.1139/A2012-004

Xiao Y (2003) Variation in needle longevity of *Pinus tabulaeformis* forests at different geographic scales. Tree Physiol 23:463–471. https://doi.org/10.1093/treephys/23.7.463

Zhang Z, Babst F, Bellassen V, Frank D, Launois T, Tan K, Ciais P, Poulter B (2018) Converging climate sensitivities of European forests between observed radial tree growth and vegetation models. Ecosystems 21:410–425. https://doi.org/10.1007/s10021-017-0157-5

Zuur AF, Ieno EN, Walker N, Saveliev AA, Smith GM (2009) Mixed Effects Models and Extensions in Ecology with R (New York)

Publisher's Note Springer Nature remains neutral with regard to jurisdictional claims in published maps and institutional affiliations.